Temperature field analysis of hydraulic engineering structure with cracks based on XFEM

Z Y Huo[1,4], Y X Gan[1], X D Chen[2] and G X Qian[3]

[1]Zhejiang Ocean University, Zhoushan 316000, China
[2]Zhengzhou University, Zhengzhou 450001, China
[3]Environmental Health Management Office of Dinghai District, Zhoushan 316000, China

E-mail: 4566055@qq.com

Abstract. For the long-term exposure to temperature load, certain parts of a concrete structure have more or less cracks during their construction or operation period. Obviously, the existence of cracks disrupts the heat transmission, having a significant impact on the existed cracks, and is not conducive to operate the structure safely. Thus, it is necessary to calculate and analyze the temperature field. XFEM was introduced into the analysis of the temperature field in hydraulic structures for its unique advantage of solving discontinuous problems, in this paper. Firstly, the approximation form of the temperature field of cracked structure was analyzed and provided; and then the discrete equations for solving discontinuous temperature field was deduced, where the crack was simulated by isothermal form, namely, the temperature field is continuous but its first derivative is not continuous; and then the temperature field by XFEM was established. A numerical example of a cross shaped plate with slit was used to verify whether the proposed method is reasonable and reliable. Finally, this method is used to analyze the expansion of the cracks in the face slab of a concrete face rock-fill dam in winter. The results are consistent with the actual monitoring results.

1. Introduction

Since the 1960s, the cracks resulting from concrete hydration heat during the construction pouring process, and the cracking due to temperature load which caused by the environmental conditions and solar radiation in the operation stage, have always been the focus of world engineering scholars. A large number of engineering practices and theoretical studies show that when the temperature field changes, the thermal stress in the concrete is produced and the change of temperature load has a significant influence on the stress state of the large-volume concrete structure. The temperature stress may exceed the stress value caused by the other external loads, even greater than the total stress of the other kinds of load [1]. There are more or less cracks in the hydraulic concrete structure running under the long-term temperature load, and the existence of the cracks not only destroys the continuity of the structure, but also disturbs the propagation of heat flow. Thus, the stress concentration at the end of the crack is aggravated; it is very easy to cause new cracks or to cause the expansion of the existing cracks, which has a negative impact on the safety of the structure.

While tracking dynamic cracks by conventional finite element method, the crack-surface is required to be consistent with the element boundary, and the grid need to constantly repartition. Considering the unique advantage of the extended finite element method (XFEM) for solving

Content from this work may be used under the terms of the Creative Commons Attribution 3.0 licence. Any further distribution of this work must maintain attribution to the author(s) and the title of the work, journal citation and DOI.
Published under licence by IOP Publishing Ltd

discontinuous problems [2-8] and could avoid these shortcomings, it was introduced to solve the temperature field in this paper.

For the hydraulic concrete structure, if the temperature of the medium inner its seam is relatively large or varies little by the boundary, and the temperature of the both sides of the crack are equal (called the isothermal crack). The crack could be treated according to the isothermal crack, and the thermal conductivity of the medium in the fracture could be taken as a small value, while it is relatively low (known as adiabatic fracture). The paper firstly analysed the approximate form of the temperature field of the crack structure; secondly, describes the XFEM for the temperature field based on the basic principle of the heat conduction, and then proves the validity of the method by using the cross plate example. Ultimately, this method is used to analyse the expansion of the cracks in the face slab of a concrete face rock-fill dam in winter. The selection method of the strengthened node in the temperature field is the same as that in the displacement field in document [2,3]. That is, in the process of crack propagation, the grid of temperature field and displacement field is always the same, so that the coordination work between different grids is avoided. This is of great significance to the subsequent three field coupling study of temperature field, seepage field and stress field, and is another innovation of this paper, besides the establishment and deduction of temperature field.

2. The approximation form of the temperature field

The XFEM approximation of the temperature field of crack structure is similar to that of the displacement field [2-7], which can be expressed as

$$T^h(\boldsymbol{x}) = \sum_{i\in I} N_i(\boldsymbol{x}) T_i + \sum_{j\in J} N_j\left(\Phi(\boldsymbol{x}) - \Phi_j\right) e_j + \sum_{k\in K} N_k(\boldsymbol{x})\left(\gamma(\boldsymbol{x}) - \gamma_k\right) f_k \tag{1}$$

where, $\boldsymbol{x}$ is the coordinate vector of the point. $N_i(\boldsymbol{x})$, $N_j(\boldsymbol{x})$ and $N_k(\boldsymbol{x})$ are shape functions. T_i is the conventional degree of freedom of node temperature. e_j and f_k represent the enriched degrees of freedom of temperature at each node. $\Phi(\boldsymbol{x})$ is a split element node enriched function. $\gamma(\boldsymbol{x})$ is a tip enriched function, while Φ_j and γ_k are the node values of both respectively; I is the set of all nodes. J is the set of all element nodes that intersect with the crack. K is the set of nodes of tip elements.

The split enriched node of both the temperature mode and displacement mode use the same enriched function $\Phi(\boldsymbol{x})$, which is continuous but its first derivative is not continuous. The asymptotic temperature field at the tip of the isothermal crack can be expressed as: $T = A\sqrt{r}\cos(\theta/2)$, where A is a constant, then $\gamma(\boldsymbol{x}) = \sqrt{r}\cos(\theta/2)$ can be chosen as a tip enriched function[2].The asymptotic temperature field at the tip of the adiabatic crack can be expressed as $T = A\sqrt{r}\cos(\theta/2)$, if A is defined as a constant, $\gamma(\boldsymbol{x}) = \sqrt{r}\cos(\theta/2)$ can be chosen as a tip enriched function which is in line with the principle of displacement mode of XFEM [3].

3. The basic principle of heat conduction

3.1. The equation of heat conduction

In consideration of homogeneous and isotropic solids, the heat absorbed by a rise in temperature must be equal to the sum of the net heat from the outside and the internal hydration heat, that is, the heat balance. Thus, one has:

$$\frac{\partial T}{\partial \tau} = a\left(\frac{\partial^2 T}{\partial x^2} + \frac{\partial^2 T}{\partial y^2} + \frac{\partial^2 T}{\partial z^2}\right) + \frac{Q}{c\rho} \tag{2}$$

where, Q is the heat emitted in unit volume per unit time. c and ρ represent specific heat and density,

τ is the time, and a is called temperature coefficient. Therefore, one can consider the $a = \lambda / c\rho$, where λ represents thermal conductivity. If there is no internal heat source, the heat conduction equation of the temperature field can be rewritten as:

$$\frac{\partial T}{\partial \tau} = \frac{\partial^2 T}{\partial x^2} + \frac{\partial^2 T}{\partial y^2} + \frac{\partial^2 T}{\partial z^2} \tag{3}$$

3.2. Boundary value conditions

In order to determine the required temperature field, it is necessary to know the initial conditions and boundary conditions. The initial transient temperature distribution is usually considered as a constant. When it is satisfied the condition, one has the following form:

$$T(x, y, z, 0) = T_0 = \text{ constant} \tag{4}$$

The boundary conditions can be divided into four types:

First boundary condition: the function $T=f(\tau)$ of the surface temperature of the concrete with time is known. When the surface temperature is equal to the known water temperature, the contact between concrete and water is satisfied with the boundary condition.

Second boundary condition: the function of the quantity of heat flow of the surface of the concrete (q) with time is known:

$$q = -\lambda \frac{\partial T}{\partial n} = f(\tau) \tag{5}$$

where n is an outward exterior normal direction. When the surface is adiabatic, it can be assumed $\frac{\partial T}{\partial n} = 0$.

Third boundary condition: one can suppose that the quantity of heat flow of the surface of the concrete (q) is proportional to the D-value between the temperature of the surface (T) and the air temperature (T_a):

$$q = -\lambda \frac{\partial T}{\partial n} = \beta (T - T_a) \tag{6}$$

where, β is the surface heat emission coefficient. If $\beta \to \infty$, this third boundary condition is converted to the first boundary condition $T=T_a$; If $\beta=0$, it is converted into an adiabatic state $\frac{\partial T}{\partial n} = 0$.

Fourth boundary condition: when two different solids contact, such as good contact, the temperature and heat flow on the contact surface should be continuous, and the boundary conditions become:

$$T_1 = T_2, \ \lambda_1 \frac{\partial T_1}{\partial n} = \lambda_2 \frac{\partial T_2}{\partial n} \tag{7}$$

3.3. The discretization equation of XFEM

According to the variational principle, two-dimensional problems satisfying the (4~5), and without considering the internal heat source, can be equivalent to the extreme value problem of the following function.

$$I(T)=\iint_R\left\{\frac{\alpha}{2}\left[\left(\frac{\partial T}{\partial x}\right)^2+\left(\frac{\partial T}{\partial y}\right)^2\right]+\left(\frac{\partial T}{\partial t}-\frac{\partial \theta}{\partial t}\right)T\right\}dxdy+\int_{\Gamma_3}\frac{\beta}{c\rho}\left(\frac{1}{2}T^2-T_aT\right)d\Gamma \tag{8}$$

where, for the boundary Γ_1, it is satisfied the condition $T=T_a$.

The solution domain is divided into finite elements. I^e is the functional on the sub-range ΔR of the element e, which can be expressed as:

$$I^e=\iint_{\Delta R}\left\{\frac{\alpha}{2}\left[\left(\frac{\partial T}{\partial x}\right)^2+\left(\frac{\partial T}{\partial y}\right)^2\right]+\left(\frac{\partial T}{\partial t}-\frac{\partial \theta}{\partial t}\right)T\right\}dxdy+\int_{\Delta\Gamma_3}\frac{\beta}{c\rho}\left(\frac{1}{2}T^2-T_aT\right)d\Gamma \tag{9}$$

The computing grid of temperature field and the selection of crack enriched node are consistent with the displacement field and percolation field. The enriched node is still divided into two types [3], split enriched and tip enriched. The degree of freedom of each node of two types is 2, the degree of freedom of partially double enriched nodes is 3, and the degree of freedom of other conventional nodes is 1.

Each degree of freedom of the elements is expressed differentiating the formula (9). The discretized equation can be rewritten as:

$$([h]+[g])\left\{\left[\{a\}^T\{b\}^T\{c\}^T\right]^T\right\}^e+[l]\frac{\partial\left\{\left[\{a\}^T\{b\}^T\{c\}^T\right]^T\right\}^e}{\partial t}-[m]\left\{\frac{\partial\theta}{\partial t}\right\}=T_a[f] \tag{10}$$

where $[a]=\left[a_i,a_j,a_m,\ldots,a_p\right]^T$, $[b]=\left[b_i,b_j,b_m,\ldots,b_p\right]^T$, $[c]=\left[c_i,c_j,c_m,\ldots,c_p\right]^T$ represent the conventional ,the slip enriched, the tip enriched degree of freedom array of the temperature at the nodes of the elements, respectively. $[h]$ is element conductivity matrix. The integrand $[*]$ of the element $h_{ij}=\alpha\iint_{\Delta R}[*]dxdy$ can be expressed as:

$$[*]=\begin{bmatrix}h_{ij}^{aa} & h_{ij}^{ab} & h_{ij}^{ac}\\ h_{ij}^{ba} & h_{ij}^{bb} & h_{ij}^{bc}\\ h_{ij}^{ca} & h_{ij}^{cb} & h_{ij}^{cc}\end{bmatrix},\quad h_{ij}^{rs}=B_j^r\left(B_i^s\right)^T\quad (r,s=a,b,c) \tag{11}$$

where, $B_i^a=\begin{bmatrix}\frac{\partial N_i}{\partial x} & \frac{\partial N_i}{\partial y}\end{bmatrix}$, $B_i^b=\begin{bmatrix}\frac{\partial(N_i\psi_i)}{\partial x} & \frac{\partial(N_i\psi_i)}{\partial y}\end{bmatrix}$, $B_i^c=\begin{bmatrix}\frac{\partial(N_i\varphi_i)}{\partial x} & \frac{\partial(N_i\varphi_i)}{\partial y}\end{bmatrix}$.

If the third boundary condition is satisfied, $[g]$ and $[f]$ could be dispersed to matrix. The integrand $[*]$ of $g_{ij}=\frac{\beta}{c\rho}\int_{\Gamma_3}[*]d\Gamma$ in $[g]$ is as follows:

$$[*]=\begin{bmatrix}g_{ij}^{aa} & g_{ij}^{ab} & g_{ij}^{ac}\\ g_{ij}^{ba} & g_{ij}^{bb} & g_{ij}^{bc}\\ g_{ij}^{ca} & g_{ij}^{cb} & g_{ij}^{cc}\end{bmatrix},\quad g_{ij}^{rs}=G_j^rG_i^s\quad (r,s=a,b,c) \tag{12}$$

$$f_i^e=\frac{\beta}{c\rho}\int_{\Gamma_3}\{N_i\quad N_i\psi_i\quad N_i\varphi_i\}^T\,d\Gamma \tag{13}$$

$[l]$ an $[m]$ are coefficient matrix, which are dispersed from time-term. The integrand $[*]$ of $l_{ij} = \alpha \iint_{\Delta R} [*] dxdy$ in $[l]$ is as follows:

$$[*] = \begin{bmatrix} l_{ij}^{aa} & l_{ij}^{ab} & l_{ij}^{ac} \\ l_{ij}^{ba} & l_{ij}^{bb} & l_{ij}^{bc} \\ l_{ij}^{ca} & l_{ij}^{cb} & l_{ij}^{cc} \end{bmatrix}, \quad l_{ij}^{rs} = G_j^r G_i^s \quad (r,s = a,b,c) \tag{14}$$

$$m_i^e = \alpha \int_{\Gamma_3} \{N_i \quad N_i\psi_i \quad N_i\varphi_i\}^T \, d\Gamma \tag{15}$$

Where $G_i^a = N_i$, $G_i^b = N_i\psi_i$, $G_i^c = N_i\varphi_i$.

By setting the results of each element, the equation set for all the nodes in the solution domain can be rewritten as:

$$[H]\{T\} + [L]\left\{\dot{T}\right\} - [M]\left\{\frac{\partial\theta}{\partial t}\right\} = T_a[F] \tag{16}$$

where, $\{T\}$ is the temperature array of all the nodes, including enriched temperature. $\left\{\dot{T}\right\}$ is the derivative matrix of $\{T\}$. $[H]$is integral conductance matrix, of which element H_{ij} is set by each element h_{ij} and g_{ij} related to the node ***i***. $[L]$ and $[M]$ are coefficient matrix dispersed from time-term, of which element L_{ij} and M_i are set by each element $\boldsymbol{l_{ij}}$ and $\boldsymbol{m_i}$ related to the node ***i***. $[F]$ is the temperature load array formed by boundary conditions. Supposing that the temperature of each node on the first boundary is equal to the given value, the equation (16) is solved, which can obtain the temperature of all node.

4. Case study

Based on the method introduced above and the method proposed in the literature [3], the crack propagation process of a cross plate with edge slanting cracks under 4 different conditions is analyzed. The temperature and mechanical boundary conditions of each working condition are detailed in table 1. The geometric size and boundary conditions of the cross plate model are shown in figure 1(a), where L=2 m, a=0.4 m, the cracks are enriched in the adiabatic form. The angle with the horizontal axis is 45° and the incremental step is 0.3a. The material properties are: Modulus of elasticity E=2.184×105 Pa, Poisson ratio v=0.3, Temperature coefficient α=1.67×10^5/℃, where ℃ is degree centigrade.

Table 1. Different boundary conditions considered in this study.

Different conditions	Temperature condition (℃)				Tensile stress (Pa)
	AB	CD	EF	GH	AB
1	10	0	10	0	0
2	0	0	0	0	10
3	10	0	10	0	10
4	10	5	10	5	10

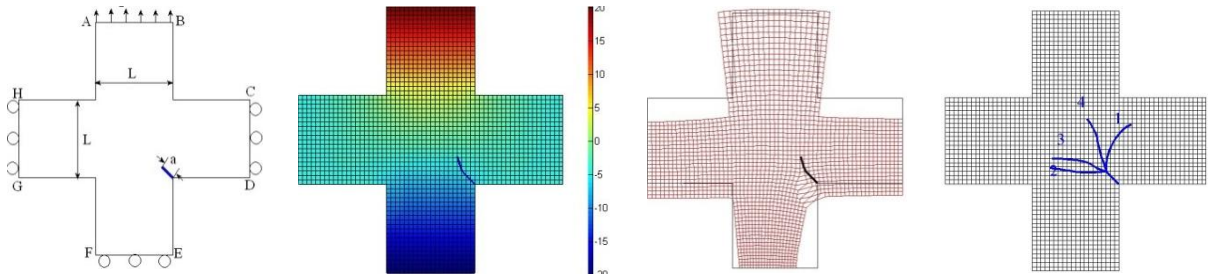


Figure 1. Model and simulation diagrams of cross plate.

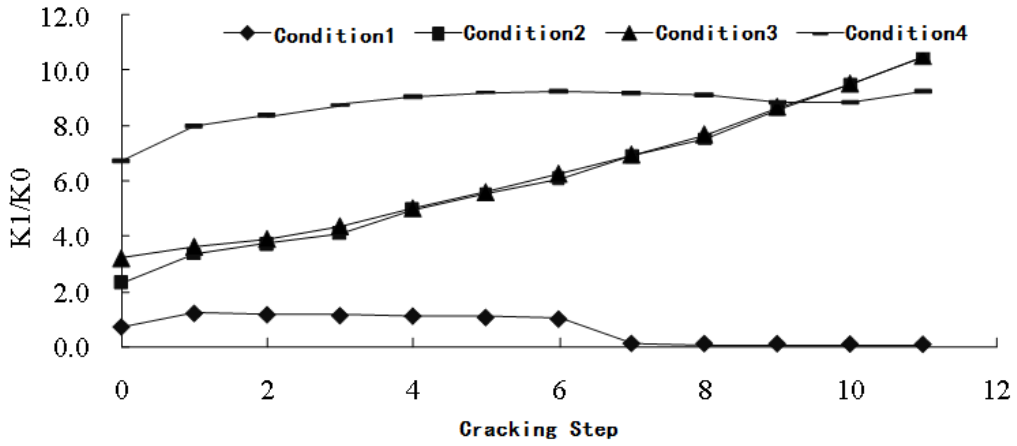


Figure 2. Variations of normalized SIFs by the crack propagation under different conditions.

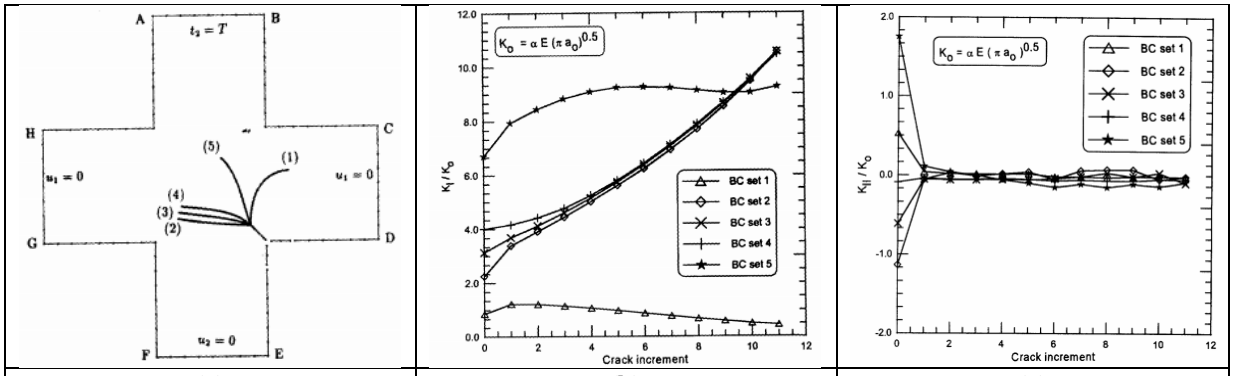
The path through 11 steps of crack propagation under four different conditions and the two types of stress intensity factors are respectively shown in figures 1(d) and 2. For the convenience of comparison, the stress intensity factor K I and K II of the type I and II crack tip are standardized with $K0=\alpha E(\pi a0)^{0.5}$. From the results of standardization shown in table 2 and the diagrams (a) and (b) in figure 2, it can be noted KI is affected by the boundary conditions greatly. On the contrary, KII is hardly affected by the boundary conditions, which tends to 0 by one step of crack propagation. Under

the condition #1, KI and KII are approximately zero after some steps of crack propagation, indicating cracks should stop expanding in real conditions. Under the condition #4, KI and KII became stable after 4 steps of crack propagation, indicating cracks should stop expanding or should be in a steady state of expansion in real conditions.

Table 2. Variations of normalized stress intensity factors (SIFs) by the crack propagation under different conditions.

SIFs	KI/K0				KΠ/K0			
step\condition	1	2	3	4	1	2	3	4
0	0.710	2.300	3.200	6.700	0.530	1.420	0.653	1.723
1	1.212	3.351	3.618	7.990	0.035	0.000	0.025	0.075
2	1.161	3.729	3.893	8.352	0.030	0.005	0.015	0.030
3	1.129	4.112	4.352	8.751	0.010	0.025	0.005	0.005
4	1.111	4.972	5.003	9.073	0.015	0.040	0.025	0.015
5	1.061	5.531	5.587	9.213	0.025	0.055	0.010	0.060
6	1.000	6.081	6.253	9.251	0.010	0.025	0.005	0.105
7	0.095	6.917	6.947	9.209	0.015	0.075	0.015	0.065
8	0.091	7.532	7.676	9.098	0.025	0.080	0.025	0.100
9	0.085	8.603	8.672	8.871	0.005	0.085	0.010	0.025
10	0.073	9.512	9.511	8.852	0.010	0.005	0.035	0.095
11	0.062	10.500	10.503	9.253	0.005	0.005	0.035	0.015

Notes: K0=αE(πa0)0.5=4.089



(a) (b) (c)

Figure 3. Results obtained in [8] considering the boundary element method (BEM).

According to figure 1(d), it can be noted the temperature load has a great impact on the path of crack propagation. The angle of the expansion path with temperature load or external force load is more than 90°.The effect of temperature and external force on the path of crack propagation is also quite different from that under single external force or temperature. Therefore, the temperature load in crack problem cannot be ignored. The diagrams (b) and the (c) in figure 1 respectively show the temperature field of 3 steps of crack propagation and displacement field magnified by 1000 times under the condition #4. The example given in the literature paper [8] is consistent with the example model in this paper, calculated by boundary element method (BEM). In particular, the different conditions 1, 2, 3, 5 correspond one by one with the different conditions 1, 2, 3, 4 in this paper. The graph of the path of crack propagation under different conditions in reference [8] and the standardization of KI and KII respectively are shown in the diagrams (a), (b) and (c) in figure 3. From

the figure, which is consistent with the results of this paper, it can be noted the effectiveness of the proposed method.

5. Engineering application

Let us consider the profile of a concrete dam. The length and crest width of the concrete face rock-fill dam are 429 m and 10 m respectively. The maximum design dam height is 139 m, and the dam crest elevation is 2010 m.a.s.l., the dam is filled with cushion layer, transition material, main pile stone, stone pile area, etc. The slab is divided into 38 parts, the length of which is about 5000 m, and the largest single block length is 218 m, of which 36 are on water slabs. The slabs aren't equal to thickness, which are from 0.3 m to 0.7 m, and the widths are all 12m. There are vertical seams between the slabs, and the surrounding joints between the slab, the toe plate and the high toe wall. The slab concrete is made of 525# ordinary portl and cement, which is two graded concrete with a labeled C25. The normal storage level of the dam is 2005 m.a.s.l., and the design and verification of flood water level are 2005 m.a.s.l. and 2008.28 m.a.s.l. respectively. After several years of operation, there are serious cracks in the concrete face slab of the rock-fill dam, and most of them are cracks that are perpendicular to the axis of the dam and distribute longitudinally on the slab. A lot of inspection results revealed many cracks are significantly affected by the temperature of concrete. There are more cracks in the slab above the reservoir water level, and cracks produced more in winter. In June 2011, the latest field inspection found 135 cracks above the water level, the longest crack extended below the 2002.0 m.a.s.l. elevation, and 129 of them were vertical cracks and 5 cracks were transverse cracks. The number of cracks increased by 12 compared with the statistics in October 2010, and the width of cracks was between 0.02 mm~0.45 mm. Therefore, it is necessary to analyze the effect of temperature change on the crack growth of the slab. The following is the analysis of the 5# slab as an example.

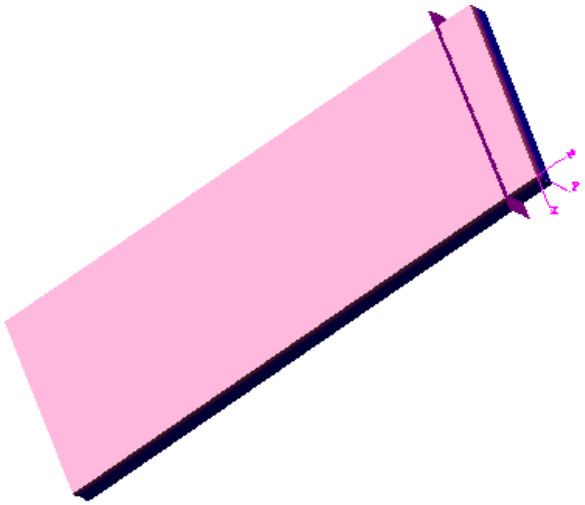


Figure 4. Profile normal to the concrete slab.

There is a longitudinal crack in the middle of the 5# panel, which extends from the 2005.5 m.a.s.l. elevation to the water level. It is found that the crack is the deepest in the 2003.5 m.a.s.l. elevation, reaching to 0.11 m deep and 0.15 mm wide. A continuous temperature drop was observed at the beginning of 2008. The XFEM was used to analyze the depth of crack growth at 2003.5 m.a.s.l. elevation during cooling. Therefore, a section is truncated along the face of the axis of the dam on the 2003.5 m.a.s.l. elevation, and an XFEM model of the section is established to analyze the expansion of the crack. The schematic diagram of section interception is shown in figure 4, where X is oriented to the width of the panel and Y to the thickness direction of the panel. It is noted that the temperature changes in the transition section and cushion layer of the operation period are relatively large, and are greatly influenced by external temperature. However, the amplitude of the thermometer measured in

the main rockfill area and the low transition zone is very small, so the simplified model ignores the influence of the temperature change in the rock-fill area. The XFEM model of the section is shown in figure 5. The model has 960 elements and 1067 nodes.

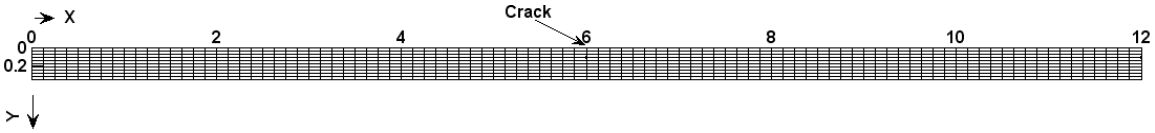


Figure 5. Mesh model of the slab profile (unit: m).

When calculating the temperature stress, only the contact problem between the extrusion wall and the panel is considered, in which the Goodman contact element is set up to simulate the contact problem between the two. The contact between the extrusion wall and the cushion is ignored, as the cushion material is dense, the extrusion wall and cushion material are well combined, and the performance of the crush wall after operation is basically the same as that of the cushion.

According to the climatic characteristics of the area of the face dam, the average temperature in the late January 2008 is the lowest in the local temperature observation data, so it is selected as the typical working condition, and the temperature change process is shown as shown in figure 6. As the temperature field between adjacent panels is less affected, the left and right sides of the panel are adiabatic when the temperature field is calculated, that is, only the heat flow perpendicular to the panel is considered, and the longitudinal flow is not considered.

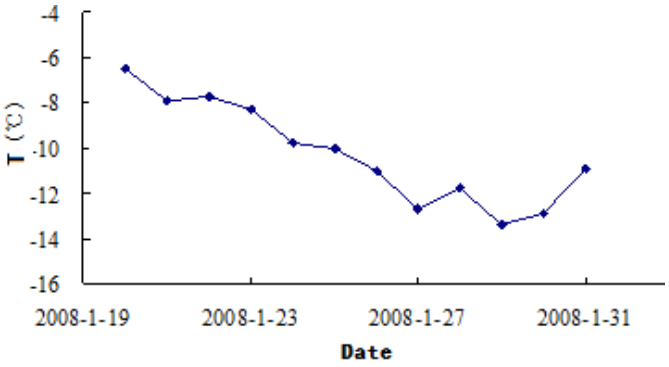


Figure 6. Temperature changes in typical working conditions.

The material parameters of slab concrete are shown in table 3. The heat exchange coefficient between concrete and air β= 2009.28 kJ/m • d • ℃, and the fracture energy G_f=120 N/m.

Table 3. Material parameters of a slab concrete.

Param	ρ (kg/m^3)	E (GPa)	μ	f_t (MPa)	Average specific heat (kJ/kg·℃)	Thermal diffusivity (m^2/d)	Thermal conductivity (kJ/m·d·℃)	linear expansivity (10^{-6}/℃)
slab	2395	22.0	0.167	1.25	0.9397	0.0903	211.92	10.05

The contact surface element stiffness coefficient is divided into normal stiffness coefficient and shear strength coefficient, According to the selection method described in [9], it can be assumed:

- Coefficient of normal stiffness. When the contact surface is compressed, a larger value should be taken to prevent the two sides of the two elements from overlapping at the contact point

(107 kN/m^3 is taken in this section). If the normal stress is calculated as the tensile stress, the smaller value of 103kN/m^3 is adopted as coefficient of normal stiffness, assuming that the contact surface cannot be pulled, so that the calculated tensile stress can be neglected.

- Coefficient of tangential stiffness. Under the action of each stage load, the value is calculated according to the empirical formula suitable for the increment method according to the stress state of the contact element.

Through the calculation of the temperature field and thermometer monitoring data of the whole working condition, it is found that the influence on slab is gradually weakening from the surface to the bottom by the temperature. The surface temperature of the panel is the same as the air temperature. The maximum temperature difference is 5.5℃ appearing in January 30, 2008.

The expansion process of slab cracks is solved by the incremental method in the winter cooling period (as shown in figure 6), and the annual average temperature of 8.5℃ is taken as the initial temperature field. It is considered that there is no stress inside the slab at this time.

The so-called increment refers to the increment of the temperature contrast initial temperature field at a certain time, which can be positive or negative. If the temperature increment is positive, indicating the temperature rise, the temperature stress will decrease (the tensile stress is positive) and vice versa, the temperature stress will increase. According to the reference [3] and assuming the temperature field at the time tn as the initial conditions, iterative computations were carried out to conclude the temperature field at the time tn+1=tn+Δt. In this way, the new temperature and stress fields are continuously obtained, and the maximum principal stress criterion is used to determine whether the fractures extend at each time step. Finally, the propagation path of the whole cooling period is obtained. The time step is taken for 1 day; by repeated trials, the crack increment is 0.01 m. The crack growth path is calculated as shown in figure 7. In January 29, 2008, the crack reached the maximum depth of 0.27 mm. Figure 8 shows the magnifying diagram of local stress map in X direction near the crack tip, when the crack is stable (on January 29, 2008).

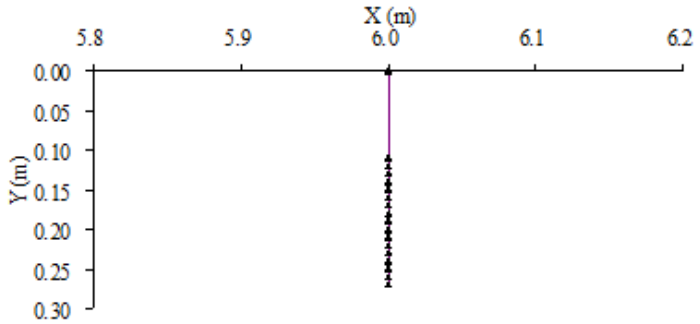


Figure 7. Crack path.

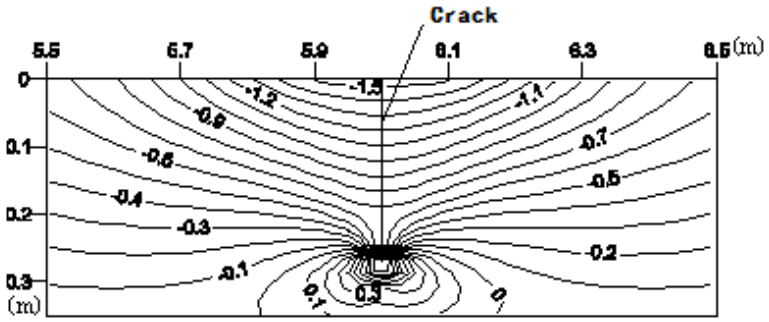


Figure 8. Distribution of stress near the crack-tip in X direction when crack being stable on January 29, 2008 (unit: MPa).

From figures 7 and 8, it is known that the tensile stress caused by the temperature drop causes the crack to extend to the cushion, and that the tensile stress has a certain stress concentration near the crack tip. As the temperature decreases, the crack expands continuously, the crack extension depth is 0.27m, which is larger than the detection value 0.03m (the detection value of the core sampling is 0.24m), and this may be due to the neglect of the three-dimensional effect and of the reinforcement in the slab. In addition, the expansion path is consistent with the monitoring results.

6. Conclusions

In view of the great influence of temperature load on the hydraulic structure of the kind of mass concrete structure, the crack expansion could have a significant negative effect. However, considering that XFEM has the unique advantage of dealing with discontinuous problems, we have used in this paper XFEM to work out the temperature field of the hydraulic structure with crack. The discrete equations for solving discontinuous temperature field was deduced, where the crack was simulated by isothermal form, namely, the temperature field is continuous but its first derivative is not continuous; then the temperature field by XFEM was established. By considering a numerical example of a cross shaped plate with slit, it was verified the proposed method is reasonable and reliable. Finally, this method is used to analyze the expansion of the cracks in the face slab of a concrete face rock-fill dam in winter. The results are consistent with the actual monitoring results.

References

[1] Gong Z X, Zhang X X, Xiao H J, *et al* 1999 *Temperature Control and Crack Prevention of Hydraulic Concrete* (Beijing: China Water Conservancy and Hydro power Press) pp 2-3
[2] Sukumar N, Chopp D L, Moes N, *et al* 2001 Modeling holes and inclusions by level sets in the extended finite-element method *Comput. Methods Appl. Mech. Eng.* **190** 6183-200
[3] Huo Z Y and Zhen D J 2010 Simulation of concrete cracking using cohesive crack model based on XFEM *Comput. Aided Eng.* **19** 29-33
[4] Dolbow J, Moes N and Belytschko T 2001 An extended finite element method for modeling crack growth with frictional contact *Comput. Methods Appl. Mech. Eng.* **190** 6825-46
[5] Khoei A R and Nikbakht M 2007 An enriched finite element algorithm for numerical computation of contact friction problems *Int. J. Mech. Sci.* **49** 183-99
[6] Moes N, Cloirec M, Cartraud P, *et al* 2003 A computational approach to handle complex micro structure geometries *Comput. Methods Appl. Mech. Eng.* **192** 3163-77
[7] Sukumar N, Chopp D L, Moes N, *et al* 2001 Modeling holes and inclusions by level sets in the extended finite-element method *Comput. Methods Appl. Mech. Eng.* **190** 6183-200
[8] Prasad N N V and Aliabadi M H 1994 Incremental crack growth in thermoelastic problems *Int. J. Fract.* **66** R45-50
[9] Yin Z Z 2007 *The Principle of Soil Mechanics* (Beijing: China Water Conservancy and Hydro power Press) pp 345-7